This is a peer-reviewed, accepted author manuscript of the following paper: Oluwasanmi, A., & Hoskins, C. (Accepted/In press). Potential use of the Diels-Alder reaction in biomedical and nanomedicine applications. *International Journal of Pharmaceutics*.

Potential use of the Diels-Alder Reaction in Biomedical and Nanomedicine Applications

Adeolu Oluwasanmi[1], Clare Hoskins[1]*

1 Department of Pure and Applied Chemistry, University of Strathclyde, Glasgow, G1 1RD, UK

*Corresponding Author: Dr Clare Hoskins, clare.hoskins@strath.ac.uk. +1415482796

Abstract: The Diels-Alder reaction and its retro breakdown has garnered increasing research focus due to several of its advantageous properties including, atomic conservation, reversibility, and substituent retention. This is especially true in biomedical application and nanomedicine development which display a preference for rapid, efficient, and clean "click" chemistry reactions allowing for delivery of active ingredients and subsequent release upon temperature elevation. There are multiple variations on the Diels-Alder based around substitution position and materials being coupled which can affect the temperature threshold for and rate of the retro reaction reversal. Hence, the Diels-Alder offers a simple coupling reaction for active ingredients with tailorable release. In this review the incorporation of the Diels-Alder chemistries and linkers within the biomedical and nanomedicine field will be discussed, as well as its use in future potential technologies.

Keywords: Diels-Alder, Drug delivery, Drug release, Intelligent delivery, Triggered release

1. Introduction

The Diels-Alder reaction was first described in 1928 by Otto Diels and Kurt Alder [1]. Their work in its discovery and development, jointly earned them the Nobel prize in Chemistry in 1950. The Diels-Alder reaction is a reversible pericyclic cycloaddition between a conjugated diene and substituted dienophile forming a substituted cyclohexene [2]. The reverse reaction, which is called retro Diels-Alder can reverse back into its original diene and dienophile, which can then form the cycloadduct again in the right conditions [3-6]. As such, the diene, dienophile and cycloadduct exist in an equilibrium determined by their current conditions.

Figure 1a shows the simplest Diels-Alder cycloaddition between 1 molecule of ethene (dienophile) and 1 molecule of 1,3-butadiene (diene) forming 1 molecule of cyclohexene with all substituents being hydrogens. Note that the molecular weights of the products are the sum of the molecular weights of their respective diene and dienophile, displaying complete conservation of all atoms in both the forward and reverse reaction. The position of every functional group is also retained in both the forward and reverse reaction shown in Figure 1b. The mechanism of the forward reaction involves the 4 π electrons (2 π bonds) of the diene and the 2 π electrons (1 π bond) of the dienophile. These π bonds break during the [4+2] pericyclic transition state forming a new π bond and 2 new sigma (σ) bonds [7].

The mechanism of the Diels-Alder reaction can be described regarding their π orbital interactions, shown in Figure 1c. The single π orbital of the dienophile and the two π orbitals of the diene, results in four possible conformations, depending on their energy [8]. Each orbital is either occupied or unoccupied by an electron at any one time. Therefore, two combinations for electron occupation with orbitals exists for the dienophile and four exist for the diene. The highest occupied molecular orbital (HOMO) is the highest energy level where electrons occupy an orbital and is lower in energy, to the lowest unoccupied molecular orbital (LUMO), which is the lowest energy level where an orbital is unoccupied [9]. For the Diels-Alder reaction to progress, the electron transfer during the reaction must occur between an occupied orbital into an unoccupied orbital. Due to the energy differences, this electron transfer occurs between the conformation for the HOMO for the dienophile and LUMO for the diene for normal $HOMO_{diene}$ interactions, where the energy gap is at its lowest and electron transfer between an occupied orbital into an unoccupied orbital can occur. $LUMO_{diene}$ controlled reactions where the HOMO is on the dienophile occur in inverse electron demand Diels-Alder reactions [10-11].

Mechanistically, the Diels-Alder reaction requires the specific arrangement of the π bonds in the diene and dienophile to occur, which allow all bond forming electron transfers to occur simultaneously. Figure 1d displays (i) the specific orientation that requires the diene to be present as its s-cis conformation, as the s-trans conformation (ii) would hinder the formation of the concerted pericyclic transition state required [12-13]. The Diels-Alder reaction possesses many characteristics that highlight its potential within a range of pharmaceutics and biomedical applications. These characteristics will be discussed further in this literature review. To summarise, the substituents and their position on the diene and dienophile impact the equilibrium conditions between the reactants and products in which lower temperatures favour the reactants and higher temperatures favour the product. Some substituents may fully impede the forward reaction, while others may render the reverse reaction impossible [1,2].
The reaction in Figure 1a between ethene and 1,4-butadiene is the simplest example of the Diels-Alder reaction, but also one of the least useful due to the relatively high activation energy required to form the cycloadduct. The type and location of substituents on the dienophile and more-so the diene affect the rate and reversibility of the Diels-Alder reaction [14]. A more commonly used Diels-Alder reaction is between substituted furans and maleimides. Studies on the effects of substituents on both the diene and dienophile have shown the Diels-Alder's reversibility is energy dependant, governed by the HOMO/LUMO energy gap, which in turn is affected by substituent effects [15].

It is the electron withdrawing effect of some substituents such as aldehydes on the diene that lowers the energy level of the reaction diene's LUMO, which leads to a lower energy gap between the diene's LUMO and dienophile's HOMO. Conversely, an electron donating group on the dienophile would raise the energy level for its HOMO which again, would reduce the energy gap facilitating the Diels-Alder reaction. The equilibrium between the reactants and cycloadduct can be determined by controlling the energy gap between the LUMO of the diene and HOMO of the dienophile with substituents.

In the case of the Diels-Alder reaction between substituted furans and maleimide, the presence of electron donating groups such as the methoxy group on the furan, favours the forward reaction compared to the unsubstituted analogue while raising the energy barrier for retro cyclization as illustrated in Figure 2. The shift in reaction equilibrium caused by substituents is due to their impact on the energy difference between the highest occupied molecular orbital (HOMO) and lowest unoccupied molecular orbital (LUMO). The Diels-Alder reaction can

produce an endo and exo isomer, which form under kinetic and thermodynamic variations of the Diels-Alder reaction respectively and potentially as a mixture, which also confers different properties to the resultant cycloadduct stereoisomers. Conversion from the endo adduct to the exo is observable even after no reactants or side/decomposition products are detected [16].

The diagram in Figure 2 demonstrates the shifting equilibrium from high endergonic (reverse favouring, forward hindered/forbidden) Diels-Alder reactions to high exergonic (forward favouring, reverse hindered/forbidden). Figure 2a shows the Diels-Alder reaction between maleic anhydride with an unsubstituted furan, which exclusively produces the thermodynamic exo isomer product, as the endo is thought to immediately undergo retro Diels-Alder. A trend of substituted furans with unsubstituted maleimide demonstrates the shifting equilibrium, starting with electron withdrawing groups such as 2-furaldehyde hindering the forward cycloaddition but favouring the retro Diels-Alder in Figure 2b, to favouring both directions with 2-methyl furan in Figure 2c. 2-methoxy furan favours the forward while hindering the reverse in Figure 2d and the forward cycloaddition of 3-ethoxy furan with maleimide being irreversible in Figure 2e [14,15]. The presence of electron donating groups such as the 3-methoxyfuran derivative in Figure 2d illustrates the high exergonicity of the subsequent Diels-Alder reaction.

During some forward Diels-Alder reactions, such as between a furan and maleimide, the retro Diels-Alder reaction is also taking place. This retro Diels-Alder has its own activation energy requirements. Within reaction conditions, the cyclisation and recyclization occur simultaneously via its endo and exo transition states at different rates, whereby, the endo isomer is the kinetically favourable product, due to its lower activation energy to form the pericyclic transition state and the higher product energy compared to the exo isomer, which also has a higher activation energy. As a result, the endo isomer will form first. The retro Diels-Alder activation energy for the endo isomer is also lower than the exo isomer. Therefore, less energy (heat) is required to form the reactants from the endo isomer [16,17]. The exo isomer is the thermodynamically favourable product due to the lower energy of the exo cycloadduct compared to the endo cycloadduct. Therefore, the exo isomer has a higher activation energy to undergo the retro Diels-Alder reaction forming the slower but more stable product [16,17]. Within reaction conditions, both isomers would form, with the endo isomer being the major product initially.

Due to the lower activation energy, recyclization of some endo cycloadducts occurs if the reaction were sufficiently warm enough, increasing with higher temperatures ultimately providing more possibilities for the exo isomer to form. Any exo cycloadducts present would undergo less recyclization compared to the endo isomer, leading to an accumulation of the exo isomer over time. If the endo isomer is the preferred product, then care must be taken to limit the recyclization during reaction conditions. Several methods describing the Diels-Alder reaction often have exceedingly long reaction times in mild conditions to achieve this [18-20]. In the Diels-Alder reactions between furan and maleimide, the cause of the endo isomers faster reaction kinetics is due to non-bond forming interactions between the electron withdrawing carbonyl pi bonds of the maleimide with the central pi bonds of the diene. Figure 3 describes how the orientation of the maleimide's carbonyls affects which isomer forms. If the carbonyls are positioned facing the central diene pi bonds, then their electron withdrawing affect is increased, lowering the activation energy, leading to a faster forming but sterically congested endo isomer. The formation of the exo isomer occurs where these carbonyls are facing away from the central diene pi bonds, which widens the energy gap between the HOMO and LUMO, leading to a slower formation. The substituents on the maleimide will face away, lowering steric congestion and leading to a more stable product.

The use of Lewis acids to catalyse the forward Diels-Alder reaction is widely known, which can shorten the long Diels-Alder reaction times that may be necessary for favouring endo enrichment of the product. Lewis acids catalyse the Diels-Alder reaction by forming a complex with the dienophile [21,22]. By forming a complex with the dienophile, the LUMO is stabilized which reduces its energy gap with the HOMO of the diene, lowering the energy barrier which favours the Diels-Alder reaction more than the uncatalyzed reaction. Heterogenous catalysis of the Diels-Alder reaction has also been reported, where porous silica with active sites doped with catalytic metals [23]. Alternatively, the Diels-Alder reaction rate can be increased by raising the pressure [24].

2. Potential of the Diels-Alder Reaction in Biomedical Applications

The Diels-Alder reaction has been utilized in a wide array of biomedical and nano based applications due to its selective, tuneable and reversibility properties. Examples of these include the use of Diels-Alder linkers as reversible conjugation points particularly in drug delivery and in the formation of self-assembled nanoparticles [25, 26]. Hydrogels fall into this

category of Diels-Alder self-assembled drug delivery vehicles, wherein hydrogels stable at physiological conditions displayed self-healing properties when damaged [27]. Chemical crosslinked hydrogels have the advantage of mechanical strength over physically crosslinked hydrogels, but often require a catalyst which may be incorporated within the hydrogel and can thus render its use unsuitable for some biomedical applications. The use of the Diels-Alder reaction to crosslink hydrogel polymer chains can proceed without the need for catalysts or initiators under aqueous conditions and can occur at physiological temperatures [28]. Hydrogels can also be utilised to encapsulate whole cells for 3D cell cultures, which are a closer representative to in vivo environments compared to traditional cell cultures in which the cells adhere to well plate walls [29].

The Diels-Alder reaction has been described as a form of click chemistry, which is a class of chemistry which can proceed under mild simple conditions with little to no by-products and simple isolation procedures [30-32]. Drugs and/or their components produced in this manner are highly sought after in drug development due to the ease of production and purification. In particularly the use of the Diels-Alder reaction is favoured, where all atoms of the reagents and product are retained. Typically, chemical reactions proceed with the formation of side products, which may require chemical scavengers or additives such as catalysers to promote the forward reaction. For example, the formation of water during an esterification reaction, requires the removal of water with dehydrating agents such as concentrated sulphuric acid. The atomic conservation property of the Diels-Alder reaction prevents the need for additives and catalysers to drive the reaction forward, which is an important advantage for biomedical applications where the purity of API's is paramount to efficacy. The Diels Alder reaction can typically proceed without the requirement of UV conditions which for biomedical applications may be advantageous, particularly with biological material such as enzymes. The emergence of side products within drug synthesis adds a layer of complexity when evaluating these drugs, as all side products must be investigated for health and efficacy effects [33-35].

The conditions shown in Table 1 display how broad the experimental conditions are for synthesizing Diels-Alder cycloadducts, which can range from several hundreds of degrees down to -78 ˚C [18]. This therefore includes milder temperatures of < 40 ˚C for preserving temperature sensitive biopharmaceutical formulations, which may contain proteins and nucleic acids. A general trend for the Diels-Alder reaction is the formation of a higher ratio of the endo isomer at lower reaction temperatures [20,35-37]. With 1,4-dioxane as the reaction solvent, the

presence of water appears to promote the endo formation arising from acrylonitrile and cyclopentadiene [38]. The reported rate constant also decreases with higher water content [38]. In contrast to this, water has also been shown to improve the reaction rate and promote the endo isomers formation [39,40]. It is thought that the presence of water stabilises the carbonyl group, which reduces the energy barrier for the forward reaction [39]. The rate boosting effect of Lewis acids on the Diels-Alder reaction is also well established, in which complexes between the dienophile and Lewis acid stabilizes the LUMO of the dienophile, which decreases the energy gap of the $HOMO_{diene}/LUMO_{dienophile}$ [41-44]. Table 2 displays additional variations of the Diels-Alder reaction for biomedical applications, centred around the choice of the diene. The furan/maleimide Diels-Alder reaction is ubiquitous throughout a wide range of nano and biomedical applications from linkers and self-assembled nanoparticles to hydrogels. This is due to the lower temperature requirements to form both the cycloadduct and undergo retro cyclisation in mild conditions and biocompatible solvents including water, making them ideal for biomedical applications. Table 2 lists three separate variations of the furan/maleimide cycloaddition for three different biomedical applications in which the Diels-Alder reaction occurs between 40-60 ˚C and undergoes retro Diels-Alder at 90-130 ˚C in water, demonstrating the mild conditions required. It has been reported that the dienophile substituent effect is remarkably smaller than the diene which has led to a near universal use of N-maleimides in furan/maleimide based Diels-Alder reactions for biomedical applications. The use of furan and structurally similar dienes, however, has a marked effect on both the forward and reverse Diels-Alder reaction onset temperatures displayed in Table 2 [4, 14].

The efficiency and atomic conserving nature of the Diels-Alder reaction serve to prevent unintended chemical interactions when utilized alongside medical applications and substances. The use of hydrogels is a promising medium for drug delivery [45-47]. These hydrogels are three-dimensional structures comprised of polymers that hold onto aqueous media that can contain dissolved materials including drug molecules, biocompatible polymers and nanoparticles. The drug release rate and permeability of these hydrogels can be modified by tuning the level of cross linking within the polymer structure [48]. The selective nature of the Diels-Alder reaction allows for the self-assembly of uniform nanoparticles that can be coupled to antibodies in mild conditions without the addition of additives and catalysts, and within the aqueous environments that promote the Diels-Alder reaction rate and stereoselectivity [49, 50]. This has given rise to poly(TMCC-co-LA)-g-PEG-furan nanoparticles. The surface of these nanoparticles are then functionalised with maleimide modified antibodies at 37 ˚C forming

self-assembled nanoparticles that allow targeted delivery to cancer cells [50]. Covalent di-sulphide bridges as well as the intermolecular and intramolecular interactions along a single peptide chain, lead to the specific protein folding observed in nature. Single chain nanoparticles (SCNP's) have historically been used to mimic this protein folding. The Diels-Alder and retro Diels-Alder reaction was used to reversibly fold and unfold SCNP's at selective regions in a manner similar to how peptide chains fold at specific regions to form the tertiary structure. SCNP's display potential as a more robust alternative to protein synthesis with reduced cost for isolation. The inclusion of highly specific diene and dienophile groups along a SCNP's is an important milestone for this goal [51]. Nanomedicine applications utilizing the Diels-Alder reaction, particularly with metallic (gold/iron/silver) nanoparticles are also firmly established in literature and show potential as future anticancer treatments.

2.1 Hydrogel Based Biomedical Applications

Wei *et al.* developed a self-healing dextran-based hydrogel that was prepared with reversible Diels-Alder reactions displayed self-healing when intentionally scratched (Figure 4) [27]. Figure 4a shows the initial generation of the hydrogel at 37 ˚C, due to the formation of cross linking via a Diels-Alder cycloaddition reaction. The ratio (R) of the dienophile, dichloromaleic-acid-modified poly(ethylene glycol) (PEG–DiCMA) and the diene, fulvene-modified hydrophilic dextran (Dex-FE) is 1, 2 and 3 in Figure 4b (i), (ii) and (iii), respectively [27].

The ratio of the diene and dienophile is shown to affect the gelation time, swelling capacity and the overall extent of cross-linking density, with negligible impact on the onset temperature for depolymerisation [30,31,52]. This resistance to changes in depolymerisation temperature is due to the use of the Diels-Alder cross linkages, which allows the hydrogel's capacity and density to be modified while retaining the physiological temperature range for activity [53]. The hydrogel discs were sliced and partially stained with rhodamine B, before being placed adjacent to unstained sliced segments. These were placed side by side at 37 ˚C, which allowed the edges to merge over time, reforming the singular hydrogel disc and allowing dye movement across the healed boundary. This healing was confirmed to be due to the formation of Diels-Alder cycloadducts across the two boundaries rather than mere surface adhesion, by lifting the hydrogel which caused it to deform under its own weight, but not split, showing that the repaired boundary could support its own weight [27]. These Diels-Alder hydrogels with self-healing activity at 37 ˚C, indicates their potential to be applied to future biomedical

applications. An onset depolymerisation temperature of approximately 37 ˚C is unlikely where most gels crosslinked via Diels-Alder cycloadducts have a Diels-Alder : retro Diels-Alder ratio of 74% at 85 ˚C and 24% at 155 ˚C, which are unsuitable for biomedical applications [54]. However, Le Châterlier's principle demonstrates that, changing the equilibrium between reagents and product in a system, such as the removal of a reagent or product, causes the system to restore the initial equilibrium. This was effectively utilized by Kirchhof *et al.* who demonstrated that the removal of the maleimide after retro Diels-Alder would shift the equilibrium to the reagents (diene and dienophile), in order to increase the generation of more maleimide, which would require a higher rate of retro Diels-Alder [55,56].

Cao *et al*. proposed a novel drug delivery method for Doxorubicin (DOX) utilizing prodrug nanogels constructed via the Diels-Alder reaction [57]. The nanogel was constructed from an alternating copolymer called Poly(styrene-alt-maleic anhydride) (PSM), a nontoxic and cheap material that is functionalised with furfuryl amine. In a single step, dithiobismaleimidoethane (DTME) as the cross linker and DOX via a hydrazone bond were incorporated. Cross linking of the polymer chains was achieved via the Diels-Alder reaction between the furfuryl amine with the maleimide groups present on DTME of other PSM chains in a one-step uncatalyzed reaction at 60 ˚C in MTBE. The primary method of cell uptake is endocytosis via endosomes, which contain acidic and reducing conditions [57]. A study into the effect of acid sensitivity on the nanogel was carried out. DOX release was shown to be 34.5% and 21.9% at pH 5.0 and 7.4 respectively in the absence of Glutathione (GSH) after 96 h. Addition of 10 mM GSH increased DOX release to 38.2% at pH 7.4 due to the disulphide cleavage caused by GSH induced reduction. At pH 5.0 with the addition of 10 mM GSH, DOX release was at 89.1% with approximately 67% occurring within the first 12 h. Overall, the result of this study shows how the action of endocytosis and incorporation in lysosomes, which also contain acidic and reducing environments, facilitates DOX release. This study was expanded to include cytotoxicity assays of the DOX Diels-Alder nanogel with MTT assays of HEK293 a kidney cancer cell line and HepG2 a liver cancer cell line. For the HEK293 cell line, the blank nanogels showed negligible effect on the cell viability between 0 – 250 μg/mL which demonstrated good biocompatibility. The presence of DOX within the nanogel reduced cell viability, with a clear correlation between nanogel concentration and cell viability reduction. The reduction in cell viability was also similar, when compared to free DOX. Some advantages of utilizing the DOX Diels-Alder nanogel is that the release of DOX can be controlled at site, under specific conditions and is mostly limited to the acidic conditions of the endosome and lysosomes after

cell uptake. A higher proportion of DOX enters cancer cells due to the EPR effect of tumours. The nanogels are also hydrophilic which helps mitigate the hydrophobic effects of the free drug [57].

Diels-Alder based hydrogels have also been used to fully encapsulate cells *in vitro* to better mimic *in vivo* conditions [58]. The *in-vitro* analysis of novel drugs and new therapies for cancer involve the growth of a cell line within cell culture flasks incubated in ideal conditions, followed by their transfer into well or culture plates, in which these cells adhere to the plate bottom. Metallic nanoparticles including those functionalised with Diels-Alder based compounds, would undergo sedimentation within these plates increasing particle and therefore Diels-Alder material concentration near the cell surface when compared to the bulk solution. Overall this would be an inaccurate situation *in vivo*. Gold nanoparticles used to treat cells present in an upright, inverted configuration has shown their cellular uptake correlated with the degree of sedimentation and was independent of other factors such as particle size, density, and concentration. This would apply to Diels-Alder functionalised gold nanoparticles as well [59-61]. This data suggests that nanoparticles formulations, which were thought to remain suspended due to Brownian motion and maintain equal concentration in the bulk and near the cell surface, did in fact undergo sedimentation [29]. To combat the issue of nanoparticle sedimentation on cells which themselves do not remain suspended, the nanoparticles and/or the cells need to remain suspended to ensure that cell uptake occurs from the bulk solution. Another study by Madl *et al*. proposed a Diels-Alder based resolution to the issue of nanoparticle sedimentation affecting cell uptake, where they opted to form hydrogels that prevent cell sedimentation [58].Here, Diels-Alder cross linked hydrogels were constructed with either furan, methyl furan, or fulvene as dienes with maleimide as the dienophile. The furan and methyl furan-based Diels-Alder hydrogels required a gelation time of 10 and 7 h respectively. The fulvene based hydrogel however, formed in less than 20 min. Human mesenchymal stromal cells (hMSC's) were encapsulated in furan, methyl furan and fulvene based nanogels, stained with a Hoechst stain for nuclei labelling and suspended in a 5% w/v aqueous solution of a 1:1 mixture of maleimide-PEG and diene-PEG to study the degree of sedimentation. Out of the three Diels-Alder hydrogels, the fulvene based hydrogel demonstrated excellent cell distribution throughout, while the furan and methyl furan-based hydrogels display cell sedimentation. The fulvene based nanogels remained stable at physiological conditions while the furan and methyl furan based nanogels slowly degraded due to the retro Diels-Alder reaction. This reversibility may not be completely disadvantageous as

some cell lines such as intestinal cell lines require a gradual hydrogel degradation in order to grow [62]. The fulvene dienes were modified with elastin-like proteins (ELP's) to aid in the binding to the cell surface and were mixed with the PEG-maleimide to form the hydrogels that encapsulated the hMSC's present. The cell viability was approximately 96% after 1 h and fell to 89 % after 7 days demonstrating a good tolerance of the initial Diels-Alder gelation mechanism and the subsequent microenvironment [58].

2.2 Nanomedicine Based Biomedical Applications

Nanomedicine is a relatively new field as a subgroup of nanotechnology. The scope of nanotechnology in medicine has focused on targeted drug delivery, wound healing, cancer treatment, and diagnostics including contrast agents to name a few [63-71]. The advantageous properties of the Diels-Alder reaction have been exploited for furthering nanomedical research and developing biomedical applications.

The Diels-Alder reaction can be used in nanotechnology particularly in drug development and design due to its advantageous properties of atom conservation in both the forward and reverse reaction, the introduction of substituents unaffected by both reactions and the cycloadducts sensitivity to temperature. As such, Diels-Alder cycloadducts within drug development are often used as controllable labile linkers [72]. The use of controllable linkers is important as it confers control over payload release *in vivo*, rather than relying on physiological activity and/or time. Within the body, these linkers will therefore need to be chemically resistant to the physiological conditions they would be present in, such as the blood stream when intravenously injected. Breakdown of these linkers would also require conditions that do not adversely affect the patient such as elevated temperatures localised to tumours in the case of anti-cancer treatments [73]. Schütz *et al.* demonstrated the Diels-Alder reversibility for nanoparticle-based applications is described in Figure 5. Here, iron oxide nanoparticles (IONP's) functionalised with either maleimides or furans, were shown to aggregate under the same conditions (60 ˚C) facilitated by the forward Diels-Alder reaction, and separating under retro Diels-Alder conditions (130 ˚C), proving the formation and breakdown of the Diels-Alder cycloadducts linkers [72]. Bulk heating of these cycloadduct functionalised IONP's facilitated linkage and separation depending on the temperature.

The use of localised heating is also possible in nanoparticle-based applications, which is important in oncological pharmaceutics, due to the requirement of such heat to be contained to

tumour sites without damaging nearby healthy tissue [73]. This is achieved by exploiting the phenomenon known as surface plasmon resonance, which is caused by the oscillations of free electrons when metal surfaces are exposed to light. Energized by their exposure to light, these electrons radiate electromagnetic waves in the infra-red region causing an increase in surface temperature [74,75]. Gold and silver are both metals that are capable of surface plasmon resonance. The use of gold nanoparticles or gold coated hybrid nanoparticles with Diels-Alder cycloadducts is firmly established in literature [76-79]. Gold is a biocompatible element that is typically unreactive but can form strong dative covalent bonds with thiols. Silver also possesses this surface plasmon resonance property to a lesser extent but does have the added benefit of antimicrobial properties [74].

Pancreatic cancer's abysmal 5-year survival rate of 7% after diagnosis makes it the 5th deadliest cancer responsible for 6% of the deaths even though it only accounted for approximately 3% of all UK cancers in 2017 [80]. A primary cause of these statistics is due to the difficulty of detecting the tumours at the earlier stages where treatment is most effective. The pancreas' position is surrounded by several important blood vessels and organs which makes surgical intervention difficult and its spread more likely [81]. Further exacerbating this is that the enhanced permeability and retention effect (EPR) is paltry or non-existent in pancreatic tumours due to stromal barriers within tumours [82]. The EPR effect is caused by the leaky vasculature of tumours due to the irregular growth of new blood vessels, which enhances their permeability to substances in the blood including cytotoxic drugs [83]. As such, current methods of administering chemotherapy led to poor uptake and activity within the tumours. The dose-limiting nature of these cytotoxic drugs renders pancreatic cancer untreatable with chemotherapy alone [84]. The disproportionate lethality of pancreatic cancer has prompted researchers to consider novel methods of treating this disease. Oluwasanmi *et al.* developed iron oxide coated in a gold shell (HNPs) which were functionalised with gemcitabine, a cytotoxic drug used to treat pancreatic cancer [85]. The surface of the HNPs was decorated with gemcitabine via a covalently bonded Diels-Alder linker with the gold surface forming a formulation called "HNP-Linker-GEM" (HLG). HLG was evaluated with *in vitro* experiments for drug release where no release was observed at room temperature, which demonstrated stability in storage conditions that was confirmed with a 4-week study at 5 ˚C and 20 ˚C where after approximately 0.3% drug release occurred in the first week with no further release observed in the subsequent 3 weeks. At 37 ˚C, approximately 15% release was observed in the first 5 min which slowly rose to approximately 17% after 60 min. In contrast,

approximately 95% release was observed at 44 ˚C over 15 min which is a large difference over a small temperature range of 7 ˚C [85,86]. The results of their *in vitro* studies in Figure 6a&b, showed that their model drug, which is maleimide containing a gemcitabine substituent (Mal-GEM) had a similar uptake to gemcitabine alone, but the HLG formation exceeded their uptake rate. At 37 ˚C, Mal-GEM's IC50 is higher than gemcitabine alone. Cells treated with gemcitabine, Mal-GEM and HLG were heated to 44 ˚C for 30 min then incubated for 48 hr. HLG demonstrated a significant decrease in IC50 for the heat-treated cells compared to their controls, which confirmed that the retro Diels-Alder mediated release of the model drug was responsible for the reduced IC50. The IC50 of released Mal-GEM from the HLG formulation 37 ˚C was higher than gemcitabine, but still significantly lower than free Mal-GEM. This is due to its better uptake. As a result of this, the heat activated HLG had a lower IC50 overall than gemcitabine, which was explained to be caused by a combination of enhanced uptake as a nanoparticle-based formulation and the heat mediated release of Mal-GEM, caused by the use of a Diels-Alder cycloadduct [85]. *In vivo*, the presence of the hybrid nanoparticles alone had negligible effect on tumour weight with and without laser irradiation when compared to the control. Dosing with gemcitabine reduced the tumour weight as expected. Dosing with HLG reduced tumour weight significantly below the control, but still above gemcitabine. It is thought the enhanced uptake facilitated this. The laser irradiation of HLG however, led to the greatest tumour shrinkage that surpassed gemcitabine's effect. The HLG formulation is also resistant to premature release due to the strong gold-thiol dative covalent bond of the Diels-Alder linker to the nanoparticle surface. Overall, this study clearly demonstrated the capabilities of utilizing Diels-Alder cycloadducts as controllable linkers [85].

Diels-Alder cycloadducts are used with nanoparticles to take advantage of their reversibility, which can be exploited for a variety of objectives not only as linkers [72,86] but also as components of drug delivery vehicles [87] and theranostics [88]. The properties of a nanoparticle-cycloadduct system hinges on the combination of nanoparticle type, size, and shape/architecture, coupled with the chosen cycloadduct. Gold nanorods functionalised with two Diels-Alder cycloadduct linkers of different chain lengths (n = 4 and n = 9) have been reported [76]. The longer chain length linker possessed increased reversibility and therefore, release of a model drug after irradiation and subsequent heat generated from the gold's surface plasmon resonance. The extent of release depended on the time of irradiation. This enhanced release was theorised to be due to the longer chains lying flat onto the surface, reducing the distance of the cycloadduct from the gold surface. The shorter chains retained their rigidity

allowing them to extend further from the surface [76]. Diels-Alder linkers were reported which were formed from 6-maleimidohexanoic acid with thiolated furans, pyrroles and thiophene at room temperatures, to maximise the proportion of endo isomers to exploit their lower stability compared to exo rich cycloadducts. These linkers were covalently attached to silver nanoparticles [89]. Typically, the pyrrole and furan dienes was more sensitive to retro Diels-Alder, where 38% and 10% reversion occurred, after 2 hr at 40 ˚C respectively, climbing to 65% and 29% at 60 ˚C, respectively. At 80 ˚C, all three dienes underwent complete retro Diels-Alder after 2 h [89].

The selective delivery of therapeutic agents to lymph nodes may pave the way in improving the effectiveness of the treatment of some clinical problems, including the clearance of viral reservoirs and destruction of B and T cell malignancies and lymph node metastases. The inherent transport barriers present within the lymph nodes restricts the accumulation of therapeutic agents. Schudel *et al*. produced a Diels-Alder based nanoparticle delivery system to improve the transport of therapeutic agents to lymph nodes which has the option of tuneable controlled release [90]. Initially poly(propylene sulphide) (PPS) nanoparticles which contain substituted dienophiles are functionalised with different thiol-reactive oxanorbornadiene (OND) variants via a Diels-Alder reaction under mild conditions (25 ˚C, in PBS at pH 7.0 – 7.4) in under 60 min. These OND variants (1, 2, 3, 4, and 5-Dn respectively) undergo retro Diels-Alder reactions at different rates which provides a tuneable release profile for the furan tagged cargo as shown in Figure 7, ranging from a half-life of approximately 17 min (1-Dn), 2.5 h (2-Dn), 10 h (d-Dn) to 29 h (4-Dn) [90]. The tuneability of the release profile was demonstrated with different molar ratios of OND variants of 8:1:1, 1:8:1, 1:1:8, and 1:1:1 of OND 1-Dn:3-Dn:4-Dn. An initial burst release of cargo was detected for all variant mixtures with the highest observed for the 8:1:1 due to the 17 min half-life of 1-Dn. The incorporation of 3-Dn and 4-Dn led to steadier release profiles which demonstrates the programmability of the OND-NP system to release its cargo over a defined duration [90].

3. The Emergence of Enzymatically Catalysed Diels-Alder Reactions

Even with all the potential advantages the Diels-Alder reaction highlights, there are several drawbacks that prevent the Diels-Alder reaction from having a wider range of industrial and medical uses. One drawback is the lack of enzyme mediated Diels-Alder reactions. Enzyme

mediated synthesis of drug compounds and their precursors is gaining increasing interest due to their advantage of high selectivity for their substrates (reducing side reactions), reusability and eliminating the requirement for toxic chemical catalysts such as transition metals. Research is emerging for the development of man-made Diels-Alder enzymes (Diels-Alderase), in which the first was reported in 2010 by Siegal *et al*. [91]. This enzyme was designed by computationally determining the atomic orientation and shape of an active site required, for a Diels-Alder reaction between 4-carboxybenzyl trans-1,3-butadiene-1-carbamate and N,N-dimethylacrylamide. The enzyme was then synthesized in genetically modified *E. Coli* cultures. In comparison with metallic catalysts, the use of the Diels-Alderase, is an order of magnitude slower, but does produce cycloadducts with a higher stereoselectivity.

Approximately 10 years after the first report of a synthetic Diels-Alderase, a naturally occurring Diels-Alderase was found in mulberry trees in 2020 [92]. This enzyme, which is called *Morus alba* Diels-Alderase (MaDA) is responsible for the synthesis of chalcomoracin, which itself has potential as an anticancer agent, due to its ability to inhibit cell proliferation and increase lung cancer cell sensitivity to radiotherapy [93]. MaDA was found to possess high substrate selectivity to the dienophile Morachalcone but catalysed pericyclic transformations with several tested dienes [92]. Other naturally occurring enzymes involved in the catalysis of the Diels-Alder reaction are TiCorS and EupF [94,95]. MaDA differs from these enzymes because it catalyses a 4+2 pericyclisation intermolecularly, while TiCorS does so intramolecularly and EupF merely catalyses the synthesis of a diene that then undergoes the Diels-Alder reaction with a dienophile [94,95]. The key advantage that MaDA provides, is that with controlled mutations, the activity and selectivity of the enzyme can be tuned to cover a wide range of Diels-Alder reactions and produce enantiomerically pure cycloadducts at lower temperatures. This is especially true for endo isomers which require longer lower temperature conditions to increase their endo product ratio [18].

4. Future Prospects and Conclusion

The numerous examples of the Diels-Alder reaction and applications described in the previous pages are but a small sample of the extensive research that has been birthed since its first description in 1928. A powerhouse in synthetic transformations that provides a plethora of chemical structures in which many are capable of efficient atomic conserving retrosynthetic reactions. With its highly established history in synthetic chemistry and other fields, there can

be no doubt that the Diels-Alder reaction will continue to see an ever-expanding role in new synthetic enterprises, particularly in the field of synthetic chemistry, pharmaceutics, biomedical sciences, polymer and material sciences. The Diels-Alder reaction is an excellent solution to the increasing demand for high speed, efficient "click" chemistry in the construction of larger repeatable polymers and dendrimers in mild conditions is already established and will likely support future synthetic efforts. This is evident in examples for both the forward and reverse reaction occurring at physiological temperatures in water without the need for UV radiation or catalysers, which is important for cell-friendly and biocompatible, click chemistry reactions. The emergence of naturally occurring and computationally derived *de novo* Diels-Alder mediating enzymes may highlight a future surge in its use, especially in the synthesis of enantiomerically pure products, especially those which have proven difficult to synthesise with current experimental conditions. Such enzymatically driven reactions may allow for highly efficient transformations without the need of higher temperatures, pressures and/or long reaction times, observed with some current procedures.

5. Acknowledgements

The authors would like to thank Tenovus Scotland (S20-05) who funded this work.

6. Authors' Contributions

AO wrote the manuscript under guidance from CH. Both authors approved the manuscript before submission.

7. Conflict of Interest

The authors would like to state there is no conflict of interest.

8. References

1. Diels O., Alder K. Synthesen in Der Hydro-Aromatischen Reihe, II. Mitteilung: Über Cantharidin. *Berichte der Dtsch*. Chem. Gesellschaft A B Ser. **1929**;*62*:554–562.
2. Borsenberger V., Howorka S. Diene-Modified Nucleotides for the Diels-Alder-Mediated Functional Tagging of DNA. *Nucleic Acids Res*. **2009**;*37*:1477–1485.
3. Rickborn B. The Retro-Diels-Alder Reaction Part II. Dienophiles with One or More Heteroatom. *In Organic Reactions*; John Wiley & Sons, Inc.: Hoboken, NJ, USA, **1998**; pp 223–629.
4. Qiu Y. Substituent Effects in the Diels-Alder Reactions of Butadienes, Cyclopentadienes, Furans and Pyroles with Maleic Anhydride. *J. Phys. Org. Chem*. **2015**;*28*:370–376.

5. Zhou J., Guimard NK., Inglis AJ., Namazian M., Lin CY., Coote ML., Spyrou E., Hilf S., Schmidt FG., Barner-Kowollik C. Thermally Reversible Diels-Alder-Based Polymerization: An Experimental and Theoretical Assessment. *Polym. Chem*. **2012**;*3*:628–639.
6. Wang B., Li Z., Liu F., Liu Y. Eco-Friendly, Self-Repairing Polymer Materials Based on Reversible Diels-Alder Chemistry. *J. Macromol. Sci. Part A Pure Appl. Chem*. **2020**;*57*:888–895.
7. Minary P., Tuckerman ME. Reaction Pathway of the [4 + 2] Diels-Alder Adduct Formation on Si(100)-2x1. *J. Am. Chem. Soc*. **2004**;*126*:13920–13921.
8. Fukui K. Role of Frontier Orbitals in Chemical Reactions. *Science*. **1982**;*218*:747–754.
9. García JI., Mayoral JA., Salvatella L. The Source of the Endo Rule in the Diels−Alder Reaction: Are Secondary Orbital Interactions Really Necessary? *European J. Org. Chem*. **2005**;*2005*: 85–90.
10. Yu S., de Bruijn HM., Svatunek D., Hamlin TA., Bickelhaupt FM. Factors Controlling the Diels-Alder Reactivity of Hetero-1,3-Butadienes. *ChemistryOpen*. **2018**;*7*:995–1004.
11. Zhang J., Shukla V., Boger DL. Inverse Electron Demand Diels-Alder Reactions of Heterocyclic Azadienes, 1-Aza-1,3-Butadienes, Cyclopropenone Ketals, and Related Systems. A Retrospective. *J. Org. Chem.* **2019**;*84*: 9397–9445.
12. Liu F., Paton RS., Kim S., Liang Y., Houk KN. Diels-Alder Reactivities of Strained and Unstrained Cycloalkenes with Normal and Inverse-Electron-Demand Dienes: Activation Barriers and Distortion/Interaction Analysis. *J. Am. Chem. Soc*. **2013**;*135*:15642–15649.
13. Saito A., Ito H., Taguchi T. Intramolecular Diels-Alder Reactions of Ester-Tethered 1,7,9-Decatrienoates: Bis[Chloro(Methyl)Aluminum]Trifluoromethanesulfonamide as a Catalyst. *Org. Lett*. **2002**;*4*:4619–4621.
14. Boutelle RC., Northrop BH. Substituent Effects on the Reversibility of Furan - Maleimide Cycloadditions. *J. Org. Chem*. **2011**;*76*:7994–8002.
15. Foster RW., Benhamou L., Porter MJ., Bučar D-K., Hailes HC., Tame CJ., Sheppard TD. Irreversible Endo -Selective Diels-Alder Reactions of Substituted Alkoxyfurans: A General Synthesis of Endo -Cantharimides. *Chem. - A Eur. J.* **2015**;*21*:6107–6114.
16. de Oliveira JC., Laborie MP., Roucoules V. Thermodynamic and Kinetic Study of Diels–Alder Reaction between Furfuryl Alcohol and N-Hydroxymaleimides — An Assessment for Materials Application. *Molecules* **2020**;*25*:2.
17. Tormena CF., Lacerda V., De Oliveg KT. Revisiting the Stability of Endo/Exo Diels-Alder Adducts between Cyclopentadiene and 1,4-Benzoquinone. *J. Braz. Chem. Soc.* **2010**;*21*:112–118.
18. da Silva Filho LC., Júnior VL., Gomes Constantino M., da Silva GVJ., Invernize PR. High Stereoselectivity on Low Temperature Diels-Alder Reactions. Beilstein *J. Org. Chem.* **2005**;*1*:14.
19. L. W. Judd, M. P. Aldred (Lomox Limited), *WO201806578 6A1*.
20. A McCluskey, J Sakoff, S Ackland, A Sim (The University Of Newcastle Research Associates Limited), *US200411082 2A1*.
21. Yates P., Eaton P. Acceleration of the Diels-Alder Reaction by Aluminum Chloride. *J. Am. Chem. Soc*. **1960**:4436–4437.
22. Fringuelli F., Piermatti O., Pizzo F., Vaccaro L. Recent Advances in Lewis Acid Catalyzed Diels−Alder Reactions in Aqueous Media. *European J. Org. Chem*. **2001**;*2001*:439–455.

23. Cantín Á., Gomez MV., De La Hoz A. Diels-Alder Reactions in Confined Spaces: The Influence of Catalyst Structure and the Nature of Active Sites for the Retro-Diels-Alder Reaction. *Beilstein J. Org. Chem*. **2016**;*12*:2181–2188.
24. Dauben WG., Kessel CR., Takemura KH. Simple, Efficient Total Synthesis of Cantharidin via a High-Pressure Diels-Alder Reaction. *J. Am. Chem. Soc*. **1980**;*102*:6893–6894.
25. Otto, S., Engberts, J.B.F.N. Hydrophobic interactions and chemical reactivity. *Org. Biomol. Chem.* **2003**;*16*:2809-2820
26. Abu-Laban, M., Kumal, R.R., Casey, J., Becca, J., LaMaster, D., Pacheco, C.N., Sykes, D.G., Jensen, L., Haber, L.H., Hayes, D.J., 2018. Comparison of thermally actuated retro-diels-alder release groups for nanoparticle based nucleic acid delivery. *J. Colloid Interface Sci.* **2018**;*526*:312–321.
27. Wei Z., Yang JH., Du XJ., Xu F., Zrinyi M., Osada Y., Li F., Chen YM. Dextran-Based Self-Healing Hydrogels Formed by Reversible Diels-Alder Reaction under Physiological Conditions. *Macromol. Rapid Commun*. **2013**;*34*:1464–1470.
28. Shi, M., Wosnick, J.H., Ho, K., Keating, A., Shoichet, M.S., 2007. Immuno-polymeric nanoparticles by Diels-Alder chemistry. *Angew. Chemie - Int. Ed*. **2007**;*46*:6126–6131.
29. Madl CM., Heilshorn SC. Rapid Diels-Alder Cross-Linking of Cell Encapsulating Hydrogels. *Chem. Mater.* **2019**;*31*:8035–8043.
30. Wei HL., Yang Z., Chen Y., Chu HJ., Zhu J., Li ZC. Characterisation of N-Vinyl-2-Pyrrolidone-Based Hydrogels Prepared by a Diels-Alder Click Reaction in Water. *Eur. Polym. J.* **2010**;*46*:1032–1039.
31. Wei HL., Yang Z., Chu HJ., Zhu J., Li ZC., Cui JS. Facile Preparation of Poly(N-Isopropylacrylamide)-Based Hydrogels via Aqueous Diels-Alder Click Reaction. *Polymer.* **2010**;*51*:1694–1702.
32. Wei HL., Yao K., Chu HJ., Li ZC., Zhu J., Shen YM., Zhao ZX., Feng YL. Click Synthesis of the Thermo- and PH-Sensitive Hydrogels Containing β-Cyclodextrins. *J. Mater. Sci.* **2012**;*47*:332–340.
33. Olsen BA., Sreedhara A., Baertschi SW. Impurity Investigations by Phases of Drug and Product Development. Trends *Anal. Chem.* **2018**;*101*:17-23.
34. Liu K-T., Chen C-H. Determination of Impurities in Pharmaceuticals: Why and How? In Quality Management and Quality Control - New Trends and Developments; *IntechOpen*, https://doi.org/10.5772/intechopen.83849.
35. Lording WJ., Fallon T., Sherburn M.S., Paddon-Row MN. The Simplest Diels–Alder Reactions Are Not Endo -Selective . *Chem. Sci.* **2020**;*11*:11915–11926.
36. Zhu J., Kell AJ., Workentin MS. A Retro-Diels-Alder Reaction to Uncover Maleimide-Modified Surfaces on Monolayer-Protected Nanoparticles for Reversible Covalent Assembly. *Org. Lett.* **2006**;*8*:4993–4996.
37. S. P. McManus, A. Kozlowski, T. L. Hutchison, B. Bray, X. Shen (Nektar Therapeutics), *US20120044422A1*.
38. Cativiela C., García JI., Gil J., Martínez RM., Mayoral JA. Salvatella L., Urieta JS.. Mainar AM., Abraham MH. Solvent Effects on Diels-Alder Reactions. the Use of Aqueous Mixtures of Fluorinated Alcohols and the Study of Reactions of Acrylonitrile. *J. Chem. Soc. Perkin Trans. 2.* **1997**; *3*:653–660.
39. Yang X., Zou J., Wang Y., Xue Y., Yang S. Role of Water in the Reaction Mechanism and Endo / Exo Selectivity of 1,3- Dipolar Cycloadditions Elucidated by Quantum Chemistry and Machine Learning. Chem. – *A Eur. J.* **2019**;*25*:8289–8303.
40. Breslow R. Hydrophobic Effects on Simple Organic Reactions in Water. *Acc. Chem. Res.* **1991**;*24*:159–164.

41. Chavan SP., Sharma P., Krishna GR., Thakkar M. I2 as an Efficient Catalyst in Ionic Diels–Alder Reactions of α,β-Unsaturated Acetals. *Tetrahedron Lett*. **2003**;*44*:3001–3003.
42. Klepp J., Sumby CJ., Greatrex BW. Synthesis of a Chiral Auxiliary Family from Levoglucosenone and Evaluation in the Diels-Alder Reaction. *Synlett* **2018**;*29*:1441–1446.
43. Vermeeren P., Hamlin TA., Fernández I., Bickelhaupt FM. How Lewis Acids Catalyze Diels–Alder Reactions. *Angew. Chemie Int. Ed*. **2020**;*59*:6201–6206.
44. Davies HML., Dai X. Lewis Acid Induced Tandem Diels-Alder Reaction/Ring Expansion as an Equivalent of a [4 + 3] Cycloaddition. *J. Am. Chem. Soc.* **2004**;*126*:2692–2693.
45. Balint R. Cassidy NJ., Cartmell SH. Conductive Polymers: Towards a Smart Biomaterial for Tissue Engineering. *Acta Biomaterialia*. **2014**;*10*:2341–2353.
46. Sivan SS., Roberts S., Urban JPG., Menage J., Bramhill J., Campbell D., Franklin VJ., Lydon F., Merkher Y., Maroudas A., Tighe BJ. Injectable Hydrogels with High Fixed Charge Density and Swelling Pressure for Nucleus Pulposus Repair: Biomimetic Glycosaminoglycan Analogues. *Acta Biomater*. **2014**;*10* : 1124–1133.
47. Işikver Y., Saraydin D. Environmentally Sensitive Hydrogels: N-Isopropyl Acrylamide/Acrylamide/ Mono-, Di-, Tricarboxylic Acid Crosslinked Polymers. *Polym. Eng. Sci.* **2015**;*55*:843–851.
48. Vermonden T., Censi R., Hennink WE. Hydrogels for Protein Delivery. *Chem Rev.* **2012**;*112*:2853-2888.
49. Abu-Laban, M., Kumal, R.R., Casey, J., Becca, J., LaMaster, D., Pacheco, C.N., Sykes, D.G., Jensen, L., Haber, L.H., Hayes, D.J. Comparison of thermally actuated retro-diels-alder release groups for nanoparticle based nucleic acid delivery. *J. Colloid Interface Sci.* **2018**; *526*:312–321.
50. Iglesias, N., Galbis, E., Romero-Azogil, L., Benito, E., Díaz-Blanco, M.J., García-Martín, M.G., De-Paz, M.V. Experimental model design: Exploration and optimization of customized polymerization conditions for the preparation of targeted smart materials by the Diels Alder click reaction. *Polym. Chem.* **2019**; *10*, 5473–5486.
51. Kramer, R.K., Belgacem, M.N., José, A., Carvalho, F., Gandini, A. Thermally reversible nanocellulose hydrogels synthesized via the furan/ maleimide Diels-Alder click reaction in water. *Int. J. Biol. Macromol*. **2019**; 141:493-498.
52. Tasdelen MA. Diels-Alder "Click" Reactions: Recent Applications in Polymer and Material Science. *Polymer Chemistry*. **2011**;*2*:2133–2145.
53. Toncelli C., De Reus DC., Picchioni F., Broekhuis AA. Properties of Reversible Diels-Alder Furan/Maleimide Polymer Networks as Function of Crosslink Density. Macromol. *Chem. Phys*. **2012**;*213*:157–165.
54. Adzima BJ., Aguirre HA., Kloxin CJ., Scott TF., Bowman CN. Rheological and Chemical Analysis of Reverse Gelation in a Covalently Cross-Linked Diels-Alder Polymer Network. *Macromolecules*. **2008**;*41*:9112-9117.
55. Kirchhof S., Brandl FP., Hammer N., Goepferich AM. Investigation of the Diels-Alder Reaction as a Cross-Linking Mechanism for Degradable Poly(Ethylene Glycol) Based Hydrogels. *J. Mater. Chem. B*. **2013**;*1*:4855–4864.
56. Kirchhof S., Strasser A., Wittmann HJ., Messmann V., Hammer N., Goepferich AM., Brandl FP. New Insights into the Cross-Linking and Degradation Mechanism of Diels-Alder Hydrogels. *J. Mater. Chem. B*. **2015**;*3*:449–457.
57. Cao XT., Vu-Quang H., Doan V.-D., Nguyen VC. One-Step Approach of Dual-Responsive Prodrug Nanogels via Diels-Alder Reaction for Drug Delivery. *Colloid Polym. Sci.* **2021**; *299*:1–9.

58. Cho EC., Zhang Q., Xia Y. The Effect of Sedimentation and Diffusion on Cellular Uptake of Gold Nanoparticles. *Nat. Nanotechnol.* **2011**;*6*:385–391.
59. Vetterlein C., Vásquez R., Bolaños K., Acosta GA., Guzman F., Albericio F., Celis F., Campos M., Kogan MJ., Araya E. Exploring the Influence of Diels–Alder Linker Length on Photothermal Molecule Release from Gold Nanorods. *Colloids Surfaces B Biointerfaces* **2018**;*166*:323–329.
60. Ghiassian S., Gobbo P., Workentin MS. Water-Soluble Maleimide-Modified Gold Nanoparticles (AuNPs) as a Platform for Cycloaddition Reactions. *European J. Org. Chem*. **2015**;*2015*:5438–5447.
61. Cadoni E., Rosa-Gastaldo D., Manicardi A., Mancin F., Madder A. Exploiting Double Exchange Diels-Alder Cycloadditions for Immobilization of Peptide Nucleic Acids on Gold Nanoparticles. *Front. Chem.* **2020**;*8*:1-4.
62. Gjorevski N., Sachs N., Manfrin A., Giger S., Bragina ME., Ordóñez-Morán P., Clevers H., Lutolf MP. Designer Matrices for Intestinal Stem Cell and Organoid Culture. *Nature.* **2016**;*539*:560–564.
63. Shi X., Sun K., Baker JR. Spontaneous Formation of Functionalized Dendrimer-Stabilized Gold Nanoparticles. *J. Phys. Chem. C*. **2008**;*112*:8251–8258.
64. Bernardi RJ., Lowery AR., Thompson PA., Blaney SM., West JL. Immunonanoshells for Targeted Photothermal Ablation in Medulloblastoma and Glioma: An in Vitro Evaluation Using Human Cell Lines. *J. Neurooncol*. **2008**;*86*:165–172.
65. Xu HL., Chen PP., ZhuGe DL., Zhu QY., Jin BH., Shen BX., Xiao J., Zhao YZ. Liposomes with Silk Fibroin Hydrogel Core to Stabilize BFGF and Promote the Wound Healing of Mice with Deep Second-Degree Scald. *Adv. Healthc. Mater*. **2017**;*6*:19.
66. Choi JU., Lee SW., Pangeni R., Byun Y., Yoon IS., Park JW. Preparation and in Vivo Evaluation of Cationic Elastic Liposomes Comprising Highly Skin-Permeable Growth Factors Combined with Hyaluronic Acid for Enhanced Diabetic Wound-Healing Therapy. *Acta Biomater*. **2017**;*57*:197–215.
67. Mofazzal Jahromi MA., Sahandi Zangabad P., Moosavi Basri SM., Sahandi Zangabad K., Ghamarypour A., Aref AR., Karimi M., Hamblin MR. Nanomedicine and Advanced Technologies for Burns: Preventing Infection and Facilitating Wound Healing. *Adv. Drug Deliver. Rev*. **2018**;*123*:33–64.
68. Qu MH., Zeng RF., Fang S., Dai QS., Li HP., Long JT. Liposome-Based Co-Delivery of SiRNA and Docetaxel for the Synergistic Treatment of Lung Cancer. *Int. J. Pharm*. **2014**;*474*:112–122.
69. Ahmad A. Wang Z. Ali R. Maitah MY., Kong D., Banerjee S., Padhye S., Sarkar FH. Apoptosis-Inducing Effect of Garcinol Is Mediated by NF-KB Signaling in Breast Cancer Cells. *J. Cell. Biochem*. **2010**;*109*:6.
70. Bar-Shalom R., Yefremov N., Guralnik L., Gaitini D., Frenkel A., Kuten A., Altman H., Keidar Z., Israel,O. Clinical Performance of PET/CT in Evaluation of Cancer: Additional Value for Diagnostic Imaging and Patient Management. *J Nucl Med.* **2003**;*44*:1200–1209.
71. Adam MJ., Wilbur DS. Radiohalogens for Imaging and Therapy. *Chem. Soc. Rev.* **2005**;*34*:153–163.
72. Schütz MB., Lê K., Ilyas S., Mathur S. Reversible Covalent Assembly of Nanoparticles through On-Surface Diels-Alder Reaction. *Langmuir*. **2020**;*36*:1552–1558.
73. Vigderman L., Zubarev ER. Therapeutic Platforms Based on Gold Nanoparticles and Their Covalent Conjugates with Drug Molecules. *Adv. Drug Deliver. Rev*. **2013**;*65*:663–676.

74. Amendola V., Pilot R., Frasconi M., Maragò OM., Iatì MA. Surface Plasmon Resonance in Gold Nanoparticles: A Review. *J.Physics Condensed Matter*. **2017**;*29*:203002.
75. Verma S., Tirumala Rao B., Rai S., Ganesan V., Kukreja LM. Influence of Process Parameters on Surface Plasmon Resonance Characteristics of Densely Packed Gold Nanoparticle Films Grown by Pulsed Laser Deposition. *Appl. Surf. Sci*. **2012**;*258*:4898–4905.
76. Vetterlein C., Vásquez R., Bolaños K., Acosta GA., Guzman F., Albericio F., Celis F., Campos M., Kogan MJ., Araya E. Exploring the Influence of Diels–Alder Linker Length on Photothermal Molecule Release from Gold Nanorods. *Colloids Surfaces B Biointerfaces* **2018**;*166*:323–329.
77. Ghiassian S., Gobbo P., Workentin MS. Water-Soluble Maleimide-Modified Gold Nanoparticles (AuNPs) as a Platform for Cycloaddition Reactions. *European J. Org. Chem*. **2015**;*2015*:5438–5447.
78. Cadoni E., Rosa-Gastaldo D., Manicardi A., Mancin F., Madder A. Exploiting Double Exchange Diels-Alder Cycloadditions for Immobilization of Peptide Nucleic Acids on Gold Nanoparticles. *Front. Chem.* **2020**;*8*:1-4.
79. Zhu J., Hiltz J., Lennox RB., Schirrmacher R. Chemical Modification of Single Walled Carbon Nanotubes with Tetrazine-Tethered Gold Nanoparticles via a Diels-Alder reaction. *Chemical Communications*. **2013**;*49*:10275-10277
80. Pancreatic cancer statistics | Cancer Research UK https://www.cancerresearchuk.org/health-professional/cancer-statistics/statistics-by-cancer-type/pancreatic-cancer#heading-Two (accessed Nov 21, 2020).
81. Bruynzeel AME., Lagerwaard FJ. The Role of Biological Dose-Escalation for Pancreatic Cancer. *Clin Transl Radiat Oncol*. **2019**;*1*:128–130.
82. Oluwasanmi A., Al-Shakarchi W., Manzur A., Aldebasi MH., Elsini RS., Albusair MK., Haxton KJ., Curtis ADM., Hoskins C. Diels Alder-Mediated Release of Gemcitabine from Hybrid Nanoparticles for Enhanced Pancreatic Cancer Therapy. *J. Control. Release* **2017**;*266*:355–364.
83. Froidevaux V., Borne M., Laborbe E., Auvergne R., Gandini A., Boutevin B. Study of the Diels-Alder and Retro-Diels-Alder Reaction between Furan Derivatives and Maleimide for the Creation of New Materials. *RSC Adv*. **2015**;*5*:37742–37754.
84. Erno Z., Asadirad AM., Lemieux V., Branda NR. Using Light and a Molecular Switch to "lock" and "Unlock" the Diels-Alder Reaction. *Org. Biomol. Chem*. **2012**;*10*: 2787–2792.
85. Wiessler M., Hennrich U., Pipkorn R., Waldeck W., Cao L., Peter J., Ehemann V., Semmler W., Lammers T., Braun K. Theranostic CRGD-BioShuttle Constructs Containing Temozolomide- and Cy7 For NIR-Imaging and Therapy. *Theranostics.* **2012**;*1*:381–394.
86. Abu-Laban M., Kumal RR., Casey J., Becca J., LaMaster D., Pacheco CN., Sykes DG., Jensen L., Haber LH., Hayes DJ. Comparison of Thermally Actuated Retro-Diels-Alder Release Groups for Nanoparticle Based Nucleic Acid Delivery. *J. Colloid Interface Sci*. **2018**;*526*:312–321.
87. Schudel A., Chapman AP., Yau MK., Higginson CJ., Francis DM., Manspeaker MP., Avecilla ARC., Rohner NA., Finn MG., Thomas SN. Programmable Multistage Drug Delivery to Lymph Nodes. *Nat. Nanotechnol*. **2020**;*15*:491–499.
88. Siegel JB., Zanghellini A., Lovick HM., Kiss G., Lambert AR., St.Clair JL., Gallaher JL., Hilvert D., Gelb MH., Stoddard BL., Houk KN., Michael FE., Baker D. Computational Design of an Enzyme Catalyst for a Stereoselective Bimolecular Diels-Alder Reaction. *Science*. **2010**;*329*:309–313.

89. Gao L., Su C., Du X., Wang R., Chen S., Zhou Y., Liu C., Liu X., Tian R., Zhang L., Xie K., Chen S., Guo Q., Guo L., Hano Y., Shimazaki M., Minami A., Oikawa H., Huang N., Houk KN., Huang L., Dai J., Lei X. FAD-Dependent Enzyme-Catalysed Intermolecular [4+2] Cycloaddition in Natural Product Biosynthesis. *Nat. Chem*. **2020**;*12*:620–628.
90. Zhang S., Zhang X., Liang J., Fang H., Huang H., Zhao Y., Chen X., Ma S. Chalcomoracin Inhibits Cell Proliferation and Increases Sensitivity to Radiotherapy in Human Non-Small Cell Lung Cancer Cells via Inducing Endoplasmic Reticulum Stress-Mediated Paraptosis. *Acta Pharmacol. Sin.* **2020**;*41*:825–834.
91. Siegel JB., Zanghellini A., Lovick HM., Kiss G., Lambert AR., St.Clair JL., Gallaher JL., Hilvert D., Gelb MH., Stoddard BL., Houk KN., Michael FE., Baker D. Computational Design of an Enzyme Catalyst for a Stereoselective Bimolecular Diels-Alder Reaction. *Science.* **2010**;*329*:309–313.
92. Gao L., Su C., Du X., Wang R., Chen S., Zhou Y., Liu C., Liu X., Tian R., Zhang L., Xie K., Chen S., Guo Q., Guo L., Hano Y., Shimazaki M., Minami A., Oikawa H., Huang N., Houk KN., Huang L., Dai J., Lei X. FAD-Dependent Enzyme-Catalysed Intermolecular [4+2] Cycloaddition in Natural Product Biosynthesis. *Nat. Chem.* **2020**;*12*:620–628.
93. Zhang S., Zhang X., Liang J., Fang H., Huang H., Zhao Y., Chen X., Ma S. Chalcomoracin Inhibits Cell Proliferation and Increases Sensitivity to Radiotherapy in Human Non-Small Cell Lung Cancer Cells via Inducing Endoplasmic Reticulum Stress-Mediated Paraptosis. *Acta Pharmacol. Sin.* **2020**;*41*:825–834.
94. Farrow SC., Kamileen MO., Caputi L., Bussey K., Mundy JEA., McAtee RC, Stephenson CRJ., O'Connor SE. Biosynthesis of an Anti-Addiction Agent from the Iboga Plant. *J. Am. Chem. Soc*. **2019**;*141*:12979–12983.
95. Chen Q., Gao J., Jamieson C., Liu J., Ohashi M., Bai J., Yan D., Liu B., Che Y., Wang Y., Houk KN., Hu Y. Enzymatic Intermolecular Hetero-Diels-Alder Reaction in the Biosynthesis of Tropolonic Sesquiterpenes. *J. Am. Chem. Soc*. **2019**:*141*:14052–14056.

Figures Legends

Figure 1. Reaction scheme displaying the simplest Diels-Alder cycloaddition between a diene and dienophile (a) and an analogous reaction (b) using a substituted diene and dienophile. (c) Illustration depicting the energy levels from low to high for the π orbitals within the dienophile (i), diene (ii) and the interaction between their LUMO and HOMO orbitals, respectively during the reaction transition state, as shown in (iii) between ethene and 1,3-butadiene. (d) Illustration of the pericyclic transition state of the Diels-Alder reaction with a diene in s-cis conformation (i) highlighting how the s-trans conformation (ii) prevents this.

Figure 2. Illustration of substituent effects on the reactivity and reversibility of the Diels-Alder reaction between substituted furans and maleimides. Only the exo product is formed in the Diels-Alder reaction between furan and maleic anhydride due to the rapid retro Diels-Alder that is occurring simultaneously. With regards to the equilibrium for reversibility of different substituted furans, the trend ranges from (ii) electron withdrawing groups (aldehydes) favouring retro Diels-Alder, to (iii) alkyl groups favouring both directions, and electron donating groups (methoxy) favouring the forward reaction. In extreme cases (d), the conditions for the retro Diels-Alder are unachievable with conventional means leading to irreversible Diels-Alder reactions.

Figure 3. Illustration of the maleimide carbonyls physical orientation during approach with the diene, and how it affects endo vs exo formation where (a) the carbonyl's are positioned under/above the diene enhancing their electron withdrawing effects forming the kinetic yet sterically hindered endo isomer. In contrast, (b) if the carbonyl groups are facing away from the diene then the less congested but slower forming exo isomer is the result.

Figure 4. Diagram illustrating the formation of the hydrogel structure at 37 ˚C (a). The ratio between dichloromaleic-acid-modified poly(ethylene glycol) (dienophile) and the fulvene-modified hydrophilic dextran (diene) is 1, 2 and 3 for b (i), (ii) and (iii) respectively. A rhodamine (red) and undyed gel disc (c) were sliced (d) different coloured semicircles placed together (iii) at 37 C, which facilitated the halves to merge, permit dye movement across the boundary and possess the ability to support the gels weight (iv).

Figure 5. Diagram describing the process where iron oxide nanoparticles (IONP's) are surface functionalised with either maleimides or furans.

Figure 6. Evaluation of *in vitro* studies on pancreatic cancer cells for uptake (a) and IC_{50} (b), comparing gemcitabine (GEM), nanoparticles (HNP), a model drug (Mal-GEM) and a nanoparticle/Diels-Alder linker/gemcitabine formulation (HLG) **(51)**. (c) *In vivo* evaluation of BxPC-3 xenograft models in Nu/Nu female mice (4–6 weeks old) dosed once a week at 3 mg kg−1 for 4 weeks. Comparison of tumours after excision: 1) control, 2) control with laser irradiation, 3) HNP, 4) HNP with laser irradiation, 5) GEM, 6) GEM with laser irradiation, 7) HNP-L-GEM, 8) HNP-L-GEM with laser irradiation, with the graphical data displayed (d).

Figure 7. The cargo release profile via retro Diels Alder of various NP-OND-Dn variants (n=3).

Table titles

Table 1. Table of Diels-Alder conditions: Solvents (white, orange & yellow), same diene+dienophile (yellow), homogenous catalysts (blue) and heterogenous zeolite metal complexes (purple) for comparisons, are present within each colour group.

Table 2. Table of Diels-Alder conditions: comparison of surface linker vs polymer vs hydrogel cross linker (red), effect of diene on retro Diels-Alder conditions (grey), for comparisons, are present within each colour group.

Graphical Abstract

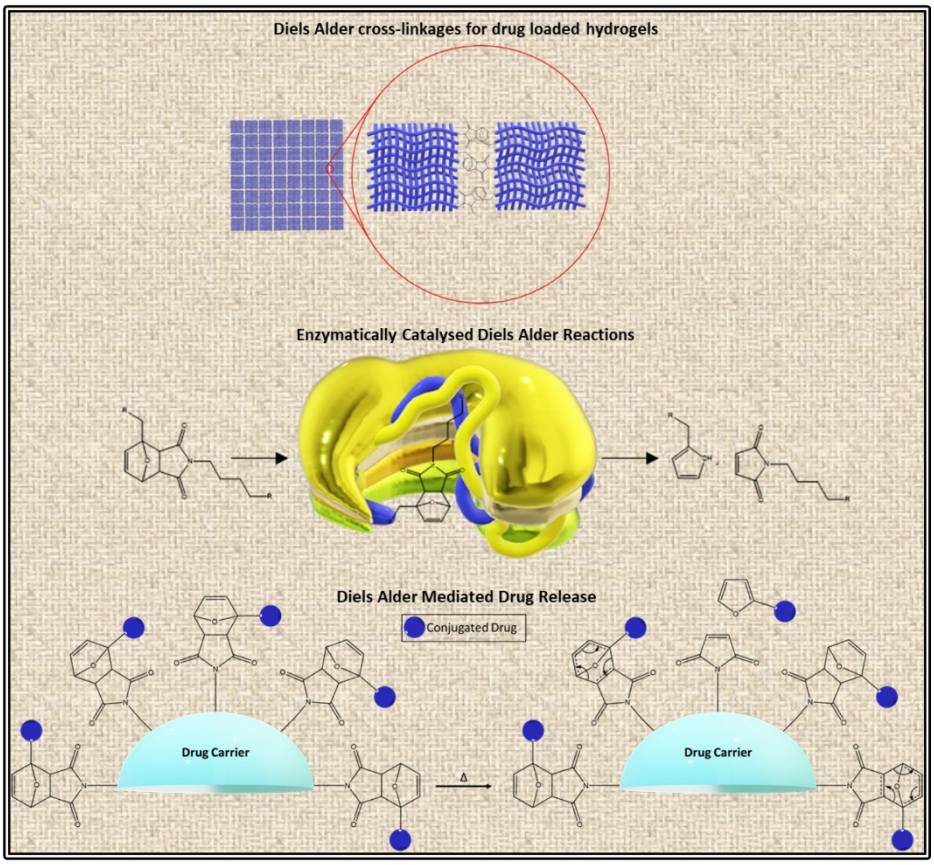

Figures

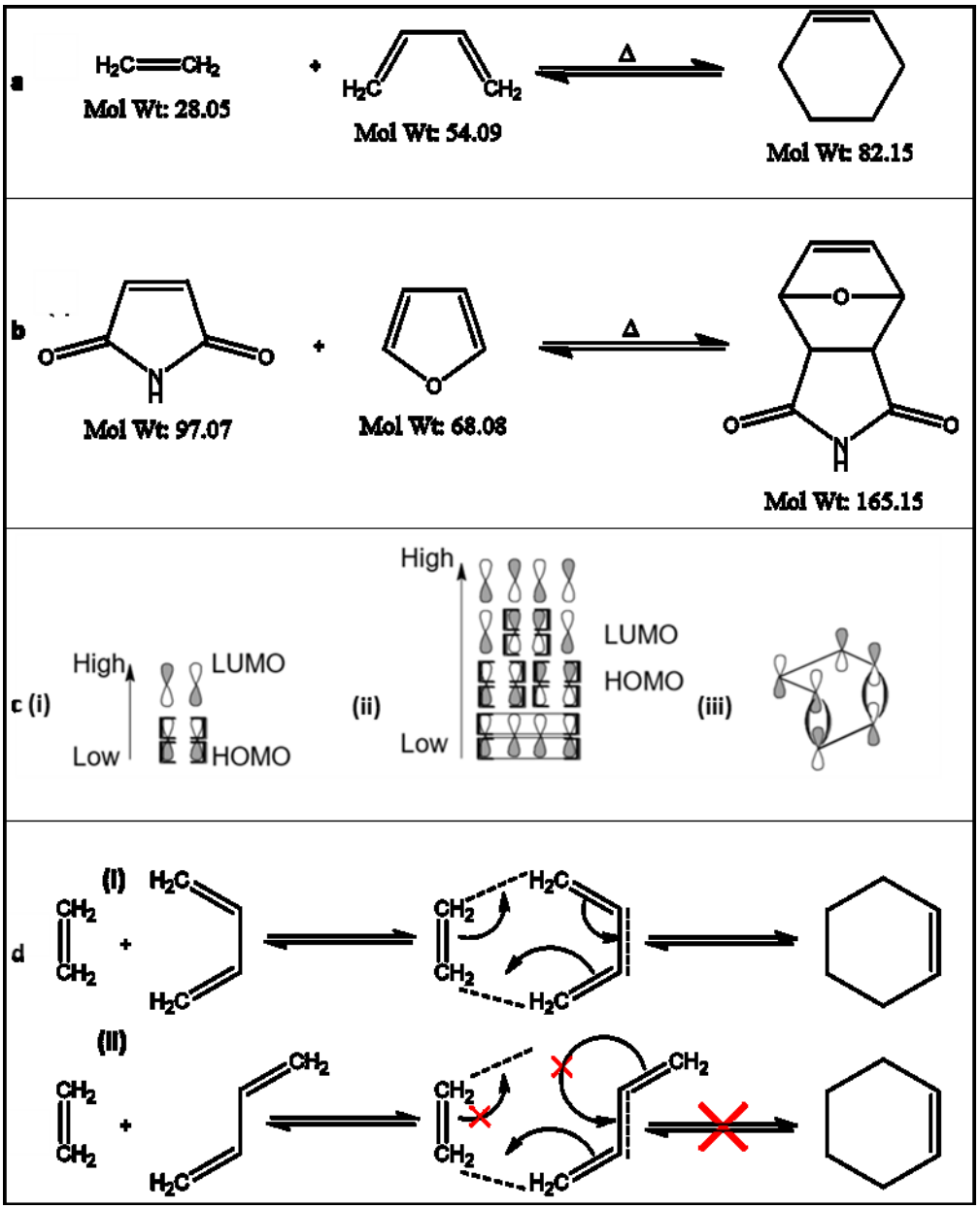

Figure 1.

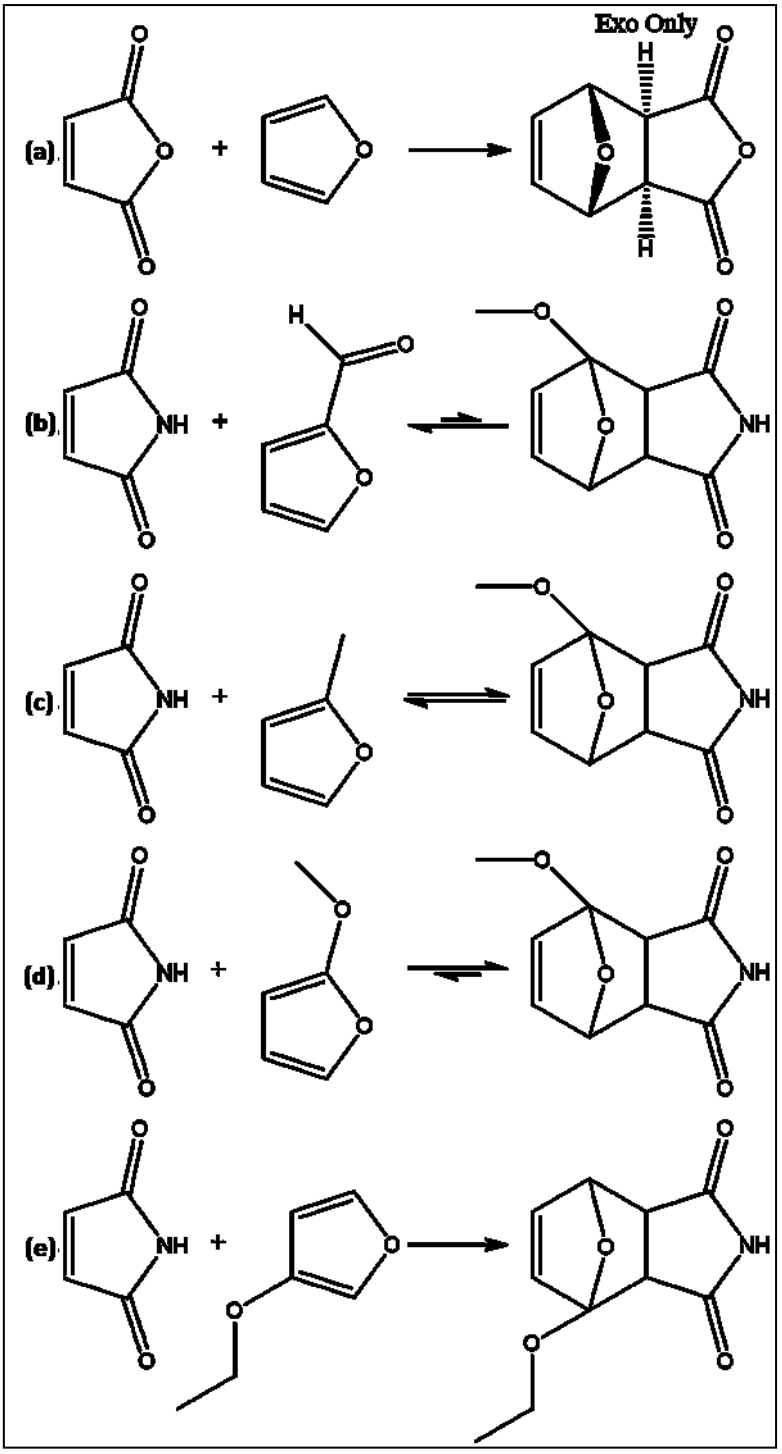

Figure 2.

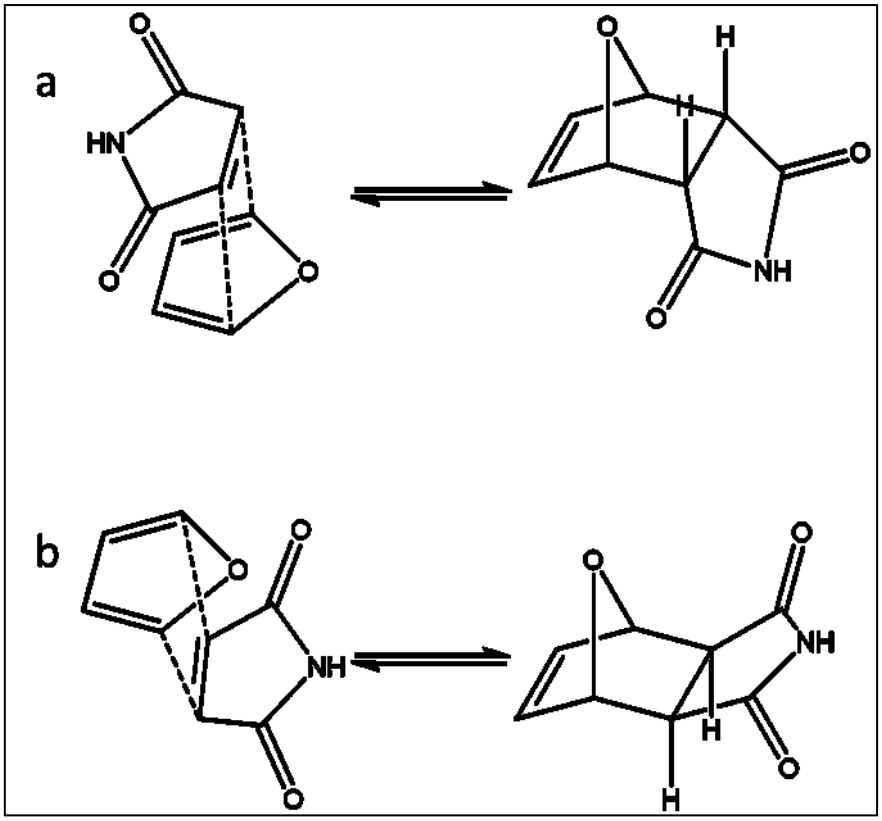

Figure 3.

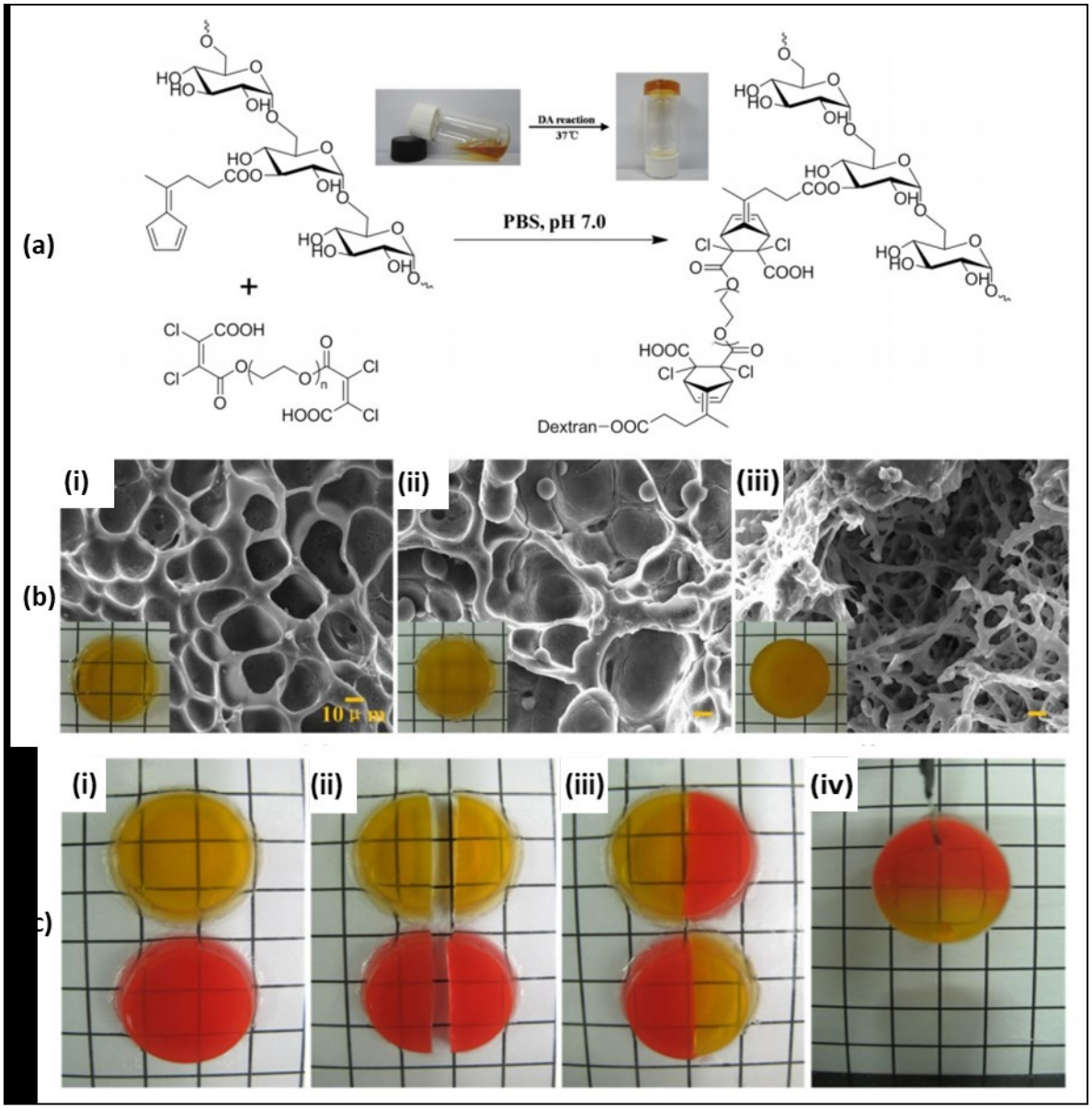
(a)
DA reaction
37℃
PBS, pH 7.0
Dextran−OOC
(b)
(i)
(ii)
(iii)
10 μm
(c)
(i)
(ii)
(iii)
(iv)

Figure 4.

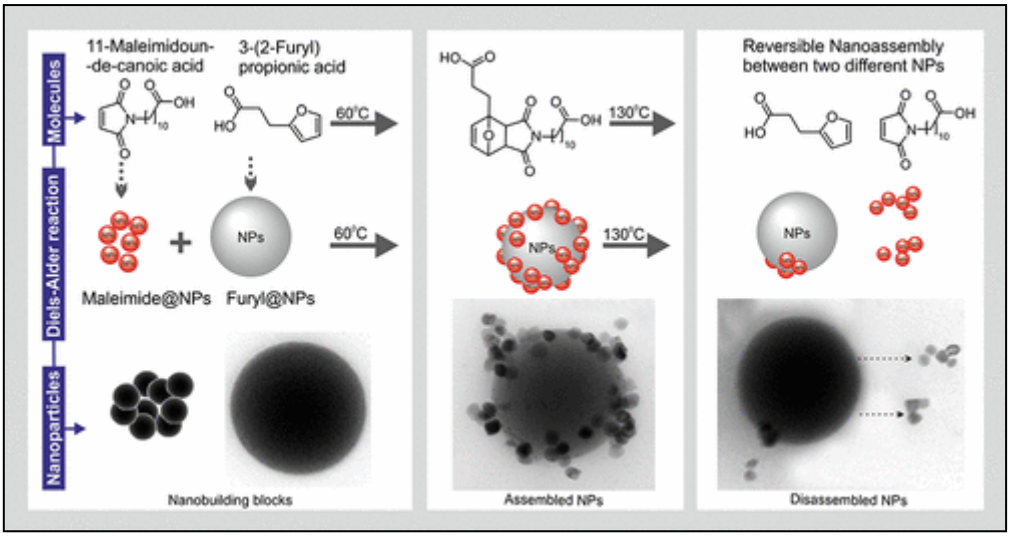

Figure 5.

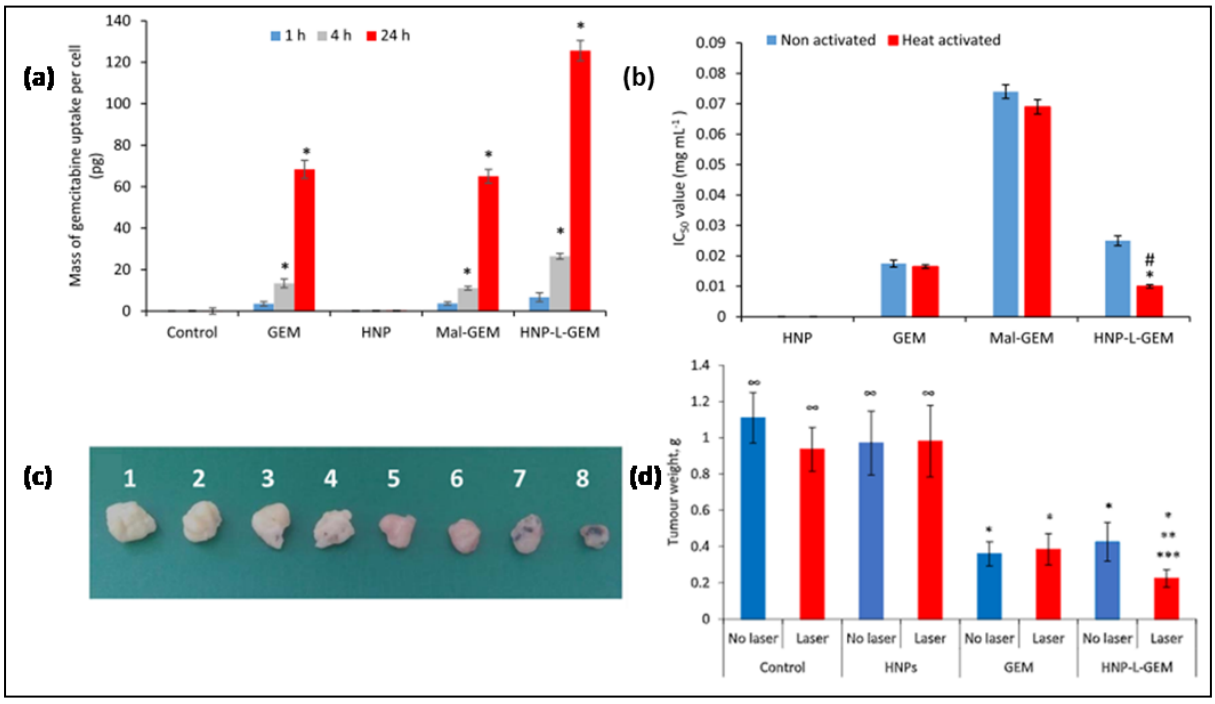

Figure 6.

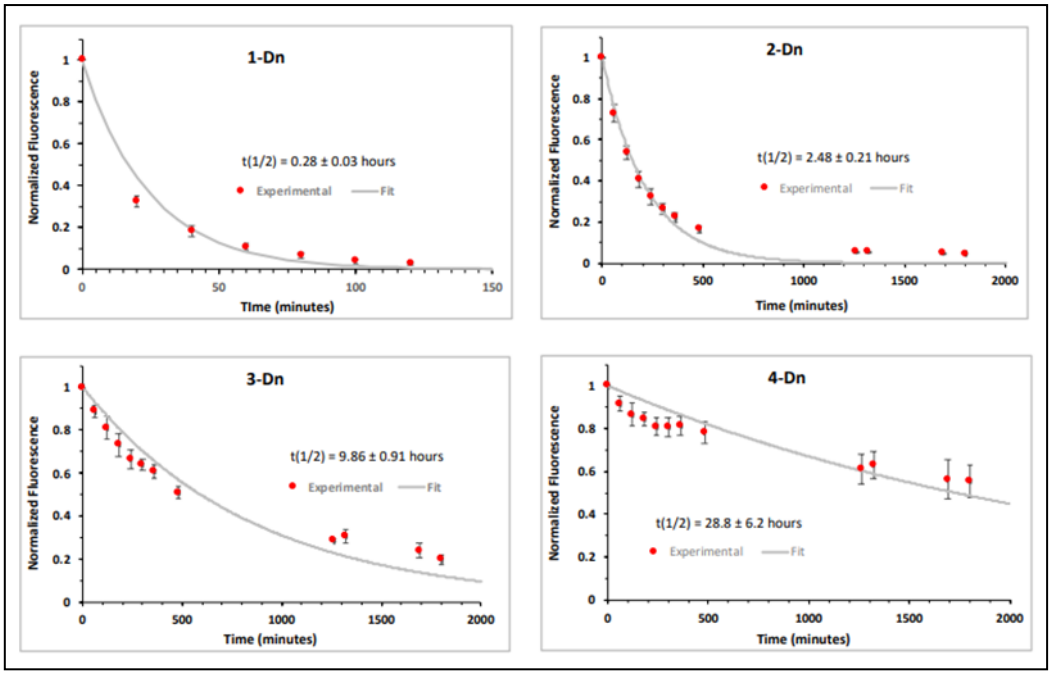
1-Dn
t(1/2) = 0.28 ± 0.03 hours
Experimental
Fit
Normalized Fluorescence
TIme (minutes)
2-Dn
t(1/2) = 2.48 ± 0.21 hours
Experimental
Fit
Normalized Fluorescence
Time (minutes)
3-Dn
t(1/2) = 9.86 ± 0.91 hours
Experimental
Fit
Normalized Fluorescence
Time (minutes)
4-Dn
t(1/2) = 28.8 ± 6.2 hours
Experimental
Fit
Normalized Fluorescence
Time (minutes)

Figure 7.

Table 1.

Solvent	Temp (°C)	Duration (h)	Yield	Endo:Exo	Ref	Variable
1,4-dioxane	30	-	-	1.45:1	(54)	H_2O (0%)
1,4-dioxane	30	-	-	1.91:1	(54)	H_2O (60%)
1,4-dioxane	30	-	-	2.08:1	(54)	H_2O (50%)
1,4-dioxane	30	-	-	2.23:1	(54)	H_2O (30%)
Benzene	-78	20	83	99:5	(53)	Temperature
Benzene	0	2	97	99:1	(53)	Temperature
Benzene	20	0.25	98	99:1	(53)	Temperature
Benzene	145	40	90	60:40	(53)	Temperature
Diethyl ether	20	168	-	66:34	(14)	Temperature
Diethyl ether	90	12	-	25:75	(14)	Temperature
Diethyl ether	100	12	62	Exo	(56)	High Temp Ether
Diethyl ether	20	70	46	63:37	(57)	Low Temp Ether
Ethyl acetate	20	20	24	1.6:1	(58)	Duration
Ethyl acetate	20	72	71	1.6:1	(13)	Duration
Dichloromethane	0	0.5	40	97:3	(59)	Iodine Catalyst
Dichloromethane	-78	2	92	98:2	(60)	$AlCl_3$
[BCl_2(1-methylimidazol)] [Al_2Cl_7] ionic liquid	0	0.25	92	98:2	(61)	[BCl_2(1-methylimidazol)] [Al_2Cl_7] ionic liquid
D-Glucose-based ionic liquid	20	1	96	8:1	(62)	D-Glucose-based ionic liquid
Dichloromethane	0	4	79	85:15	(63)	Control
Dichloromethane	0	4	92	95:5	(63)	Zeolite LiY
Dichloromethane	0	4	95	99:1	(63)	Zeolite NaY
Dichloromethane	0	4	99	99:1	(63)	Zeolite KY
Dichloromethane	0	4	99	7:3	(63)	Zeolite CsY
THF	20	48	55	74:26	[6]	H_2O (0%)
THF	40	48	65	59:41		H_2O (0%)
THF	20	48	67	70:30		H_2O (10%)
THF	40	48	>90	56:44		H_2O (10%)
THF	20	48	>90	71:29		H_2O (20%)
THF	40	48	>90	56:44		H_2O (20%)

Table 2.

Diene	Dienophile	DA Temp [˚C]	DA Duration [h]	>20% rDA Temp [˚C]	rDA Duration [h]	rDA Solvent	Ref	Variable
2-furan derivative	N-maleimide	60	48	130	24	H_2O	[66]	Surface Diels-Alder Linker (IONP's)
2-furan derivative	N-maleimide	40	48	95	N/A	H_2O	[6]	Diels-Alder Polymer
2-furan derivative	N-maleimide	60	0.5	90	1	H_2O	[7]	Diels-Alder Cross Linked Cellulose Hydrogel
2-furan derivative	N-maleimide	20	168	60	2		[8]	Surface Diels-Alder Linker (AgNP's)
2-thienyl derivative	N-maleimide	60	72	80	2		[8]	Surface Diels-Alder Linker (AgNP's)
2-pyrrole derivative	N-maleimide	60*	72	40	2		[8]	Surface Diels-Alder Linker (AgNP's)

*Forward Diels-Alder reaction conditions utilised excess maleimide to drive equilibrium to cycloadduct.